Original Article

Institution of MECHANICAL ENGINEERS

Journal of MECHANICAL ENGINEERING SCIENCE

Proc IMechE Part C:
J Mechanical Engineering Science
2019, Vol. 233(8) 2696–2712

DOI: 10.1177/0954406218796043
journals.sagepub.com/home/pic

SAGE

A comparative study of the performance of the mixed flow and radial flow variable geometry turbines for an automotive turbocharger

K Ramesh[1,2], BVSSS Prasad[1] and K Sridhara[2]

Abstract

A new design of a mixed flow variable geometry turbine is developed for the turbocharger used in diesel engines having the cylinder capacity from 1.0 to 1.5 L. An equivalent size radial flow variable geometry turbine is considered as the reference for the purpose of bench-marking. For both the radial and mixed flow turbines, turbocharger components are manufactured and a test rig is developed with them to carry out performance analysis. Steady-state turbine experiments are conducted with various openings of the nozzle vanes, turbine speeds, and expansion ratios. Typical performance parameters like turbine mass flow parameter, combined turbine efficiency, velocity ratio, and specific speed are compared for both mixed flow variable geometry turbine and radial flow variable geometry turbine. The typical value of combined turbine efficiency (defined as the product of isentropic efficiency and the mechanical efficiency) of the mixed flow variable geometry turbine is found to be about 25% higher than the radial flow variable geometry turbine at the same mass flow parameter of 1425 kg/s $\sqrt{K}$/bar m^2 at an expansion ratio of 1.5. The velocity ratios at which the maximum combined turbine efficiency occurs are 0.78 and 0.825 for the mixed flow variable geometry turbine and radial flow variable geometry turbine, respectively. The values of turbine specific speed for the mixed flow variable geometry turbine and radial flow variable geometry turbine respectively are 0.88 and 0.73.

Keywords

Turbocharger, radial flow turbine, mixed flow turbine, variable geometry, turbine performance, mixed flow variable geometry turbine

Date received: 19 September 2017; accepted: 19 July 2018

Introduction

In recent times, the automotive engines have been experiencing a demand for significant downsizing that results in the reduction of engine capacities by up to 40%.[1] The increase in such values of power-to-weight ratios requires an optimum size for the turbocharger. Whilst a turbocharger conventionally uses a radial flow geometry turbine, a turbocharger with mixed flow geometry provides increased airflow rate to enable downsizing of the engine. Further, a variable geometry caters to the demand of variation in flow rate at different engine speeds. According to Okapuu[2] and Karamanis et al.,[3,4] mixed flow geometry possesses the best features of both radial and axial flow turbines, in terms of mass flow, efficiency, and stage expansion ratio. According to Baines et al.,[5] mixed flow turbine with forward swept blades has higher mass flow and flatter characteristics and exhibits best efficiency at lower velocity ratio than the radial flow turbine. The present trend in automotive turbocharger is thus to use mixed flow turbines with the low inertia wheels. For more details, one can refer to the study of Roclawski et al.[6]

Rajoo and Martinez-Botas[7] described two possible options of mixed flow turbines as shown in Figure 1(a) and (b). Both the designs create an even-matching of exit plane of the nozzle vane with the leading edge of the mixed flow rotor. The configuration in Figure 1(a) needs chamfering of nozzle vane at the exit, whereas the configuration

[1]Turbomachines Laboratory, Department of Mechanical Engineering, Indian Institute of Technology Madras, Chennai, India
[2]Turbo Energy Private Limited, Engineering Research and Development Centre, Kancheepuram, India

Corresponding author:
K Ramesh, Turbomachines Laboratory, Department of Mechanical Engineering, Indian Institute of Technology Madras, Chennai 600 036, Tamil Nadu, India.
Email: ramesh.k@turboenergy.co.in

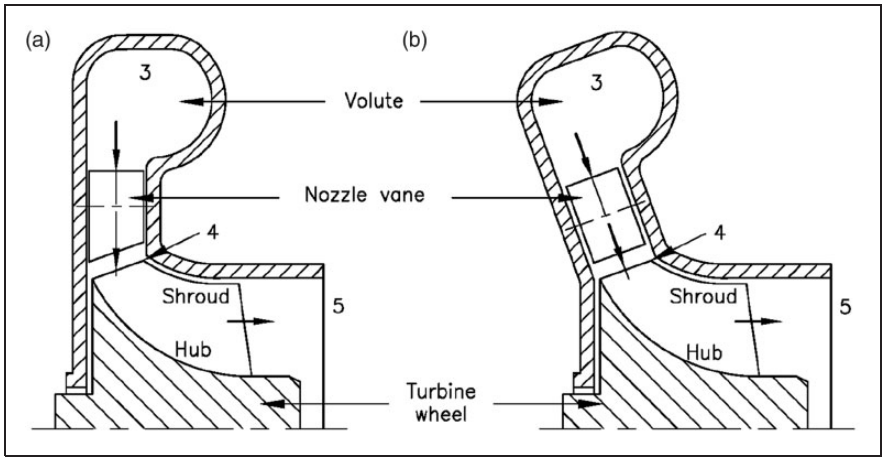

Figure 1. Possible options of nozzle vanes for a mixed flow turbine: (a) vane with flat hub/shroud surface; and (b) vane with inclined hub/shroud surface.

in Figure 1(b) needs sliding of nozzle vane on an inclined surface. Although the design of Figure 1(b) contains an "ideal" nozzle ring,[8] Rajoo and Martinez-Botas[7] adapted the design in Figure 1(a), due to the relative simplicity of the kinematic mechanism for actuating the nozzle vane. The design of Figure 1(b) was left unattended due to the complexity of the required kinematic mechanism.

In order to achieve the configuration of Figure 1(b), the authors have designed a novel kinematic mechanism (patent under preparation) wherein the nozzle vanes are arranged in a spherical plane. The gap between inner bearing (hub side) and outer bearing (shroud side) surfaces is thus maintained constant for all the nozzle vane positions. The objective of the present work is to bring out quantitative estimates of the relative performances of radial flow variable geometry turbine (RFVGT) and mixed flow variable geometry turbine (MFVGT), with the configuration shown in Figure 1(b), hitherto not assessed and reported in the literature. Table 1 summarizes the comparative features of RFVGT and MFVGT. It can be concluded from the listed features of Table 1, that the mixed flow turbine contributes towards (a) an increase in lower end engine torque with improved time to reach the targeted torque, (b) increase in the power output with reduced specific fuel consumption, (c) reduction in the overall emissions from an engine and (d) downsizing of the engine.

Choice of RFVGT and MFVGT configurations

In order to compare the performance of RFVGT and MFVGT configurations on a common platform, the geometries with almost same dimensions are chosen as in Table 2. These common geometric features are: (i) turbine housing volute area, (ii) number of nozzle vanes, (iii) number of turbine blades, (iv) turbine wheel throat area and the exit blade angle, and (v) compressor as a loading device. However, the major differences between the two are: (i) direction of flow leaving the turbine housing volute, (ii) direction of the flow entry and leaving the nozzle vanes, (iii) direction of flow entering the turbine wheel, and (iv) tip diameter of the turbine wheel.

Figure 2 shows turbine stage for RFVGT and MFVGT, which includes turbine housing, nozzle vanes, and turbine wheel. In MFVGT, the hub profile of the mixed flow turbine wheel has a larger radius. The larger hub radius combined with flow entry to the turbine wheel in a mixed flow (non-radial) direction provides a minimum change in the flow direction, and hence improvement in flow uniformity, for MFVGT. The turbine volute profile is designed for delivering the flow circumferentially towards nozzle vanes in a mixed flow direction of 20°. For both RFVGT and MFVGT, a similar nozzle vane shape is used. However, the profiles of hub and shroud sides have flat (straight) surfaces in RFVGT, whereas they are spherically shaped for MFVGT. Further, the cartridge vane bearing surfaces are also spherical in MFVGT. The use of spherical profiles with respective vane bearing rings ensures uniform clearances at inner and outer vane surfaces during opening and closing of nozzle vanes. A small gap of about 0.125 mm is maintained between nozzle vane and the bearing rings to accommodate thermal expansion.

The mixed flow angle of 20° is fixed considering the limitation on the bearing housing side to accommodate the nozzle vane actuation. Although forward swept blades are used in both RFVGT and MFVGT, the level of sweeping is higher in MFVGT and hence achieves higher turbine stage loading.[10] The tip diameters of the turbine wheel and the exducer are 30 mm and 24.75 mm and 29.12 mm and 24.75 mm for RFVGT and MFVGT, respectively. These dimensions ensure same blade width (b) at entry for both mixed flow and radial flow turbine wheels. In MFVGT, at entry to the turbine wheel, the wheel

disc is scalloped to facilitate the flow entry to the turbine wheel in a mixed flow direction. This contributes for the reduction in mass of the turbine wheel. According to He et al.,[18] this feature also reduces centrifugal stresses on the wheel disc. The exit blade angles of the turbine wheel at the mid span of the blades are 38° for both RFVGT and for MFVGT with respect to rotor axial direction. This ensures

Table 1. Comparative features of RFVGT and MFVGT.

RFVGT	MFVGT
1. Maximum turbine flow capacity is limited for the given geometry size. Higher level of turbine speed is required to achieve the required mass flow rate for the given turbine wheel tip diameter.	1. The large radii of curvature along hub and shroud in mixed flow turbine wheel helps in achieving the higher flow rate for the same tip diameter of the radial flow turbine without significant reduction in efficiency, refer to Oh et al.[9] Maximum turbine flow capacity is higher for MFVGT compared to RFVGT for the given geometry size, refer to Ramesh et al.[10]
2. Flow entry is in the radial direction only, but flow turning is from radial inlet to axial outlet. The flow turning creates secondary flow vortices, a source of loss, refer to Baines.[11]	2. Two degrees of freedom exist in the flow entry, radial, and axial directions. Less flow turning occurs in both the tangential direction and in the meridional plane (<90°) from inlet to axial outlet. Flow turning angle from entry to the exit is less than 90°. The flow in the turbine wheel is uniform, Baines.[12]
3. Higher incidence loss occurs during higher speed operation due to restriction in the direction of flow entry.	3. The incidence losses are low in mixed flow turbine due to flow entry in both radial and axial direction; refer to Oh et al.[9] and Rodgers.[13]
4. Turbine power is proportional to the mass flow rate and expansion ratio for the given turbine inlet temperature. Since the mass flow rate is generally lower for radial flow turbine, the power is also lower for RFVGT. For higher turbine power output, higher tangential velocity at inlet to the turbine wheel is required. To achieve this, the relative velocity of the gas at entry to the turbine wheel is more in the positive direction. For correct incidence, the blades must be in curved shape and this is not possible due to blade stresses, refer to Baines.[11] For maximum power output, the rotor inlet relative flow angle is large (about 43.2° for 670 kW turbine) and this is not possible with radial blades, refer to Baines.[12]	4. Since the mass flow rate is higher for the given expansion ratio and turbine inlet temperature, the turbine power is higher with mixed flow turbine for the similar size of the turbine in terms of wheel diameter and the turbine housing volute area. Power output of about 20% higher than radial turbine is possible with mixed flow turbine. For achieving higher power output, the correct incidence with the relative velocity of the gas at entry to the turbine wheel in the positive direction can be achieved with mixed flow turbine wheel with forward swept design without affecting the blade stresses, refer to Baines.[11] Mixed flow turbine improves the transfer of energy from pulsating exhaust gas to the turbine, due to non-zero blade angle and additional degrees of freedom to the flow with reduced incidence loss and the better flow development in the rotor passage.[4] Higher power generation is possible with mixed flow turbine with zero or positive swirl at the turbine inlet. In addition, it provides better transient response due to lower mass and polar moment of inertia; refer to Oh et al.[9]
5. The ratio of exducer to inlet tip diameter is limited considering that the blade stresses limit the effective turbine flow area. Sharp curvature of the hub profile in the radial turbine causes the reduction in specific speed.	5. Incoming flow has radial and axial components, less curvature in the meridional plane, contributing for high specific speed.[11] Higher mass flow rates for the same tip diameter contributes for the higher specific speed.[9]
6. During engine transient condition, the energy available to the turbine is partially used to overcome the inertia of the rotor and the remaining part is used for supplying the power to the compressor. In radial flow turbine, the mass of the rotor is high and hence the inertia is high, causing reduction in transient response, refer to Baines.[11]	
7. Peak efficiency occurs at higher expansion ratio and higher efficiency over short operating range of mass flow and expansion ratios. Lower turbine efficiency occurs at higher expansion ratios.	
8. The peak efficiency occurs at a velocity ratio of about 0.7. Due to longer blade passage, the frictional loss is high and there is reduction in power output.	

(continued)

Table 1. Continued.

RFVGT	MFVGT
	6. Turbine should deliver the higher turbine power for the given input energy over wide operating speed. This is possible with mixed flow turbine since mixed flow turbine possesses the lower moment of inertia over radial flow turbine. Rotor inertia is low and hence improvement in transient response, refer to Cox et al.[14] As per Roclawski et al.,[15] pulse flow energy utilization improves the transient response. 7. Peak efficiency occurs at lower expansion ratio and higher turbine efficiency over the wide operating range of mass flow and expansion ratios. Higher turbine efficiency also occurs at higher expansion ratio; refer to Li et al.[16] Peak efficiency is shifted towards higher expansion ratio (which correspond to lower velocity ratio), refer to Palfreyman et al.[17] 8. The peak efficiency occurs at velocity ratios lower than 0.7 due to non-radial blade inlet angle. The frictional loss is less due to shorter blade passage. Better efficiency at higher expansion ratio is observed with mixed flow turbine.[9] Higher efficiency at lower velocity ratio is observed, refer to Rodgers.[13]

MFVGT: mixed flow variable geometry turbine; RFVGT: radial flow variable geometry turbine.

Table 2. Specification for the RFVGT and MFVGT.

Description	RFVGT	MFVGT
Turbine housing volute area at reference section (mm^2)	518	515
Flow direction leaving the volute (°)	0	20
Flow direction in the VGT – nozzle channel (°)	0 (radial)	20 (mixed)
Number of vanes	9	9
Flow direction entering the turbine wheel at leading edge (°)	0 (radial flow direction)	20 (mixed flow direction)
Turbine wheel tip diameter, d_4 (mm)	30	29.12
Turbine wheel blade width at entry, b (mm)	4.5	4.5
Number of turbine blades	8	8
Exit blade angle at mid span (°)	38	38
Turbine wheel exducer throat area (mm^2)	256	256
Compressor wheel tip diameter (mm)	32.5	32.5

MFVGT: mixed flow variable geometry turbine; RFVGT: radial flow variable geometry turbine.

the similar turbine wheel exducer throat area for RFVGT and MFVGT.

Figure 3 shows the schematic of the turbine wheel used in both RFVGT and MFVGT. The entry to the turbine wheel has a forward sweep and a positive lean in both the turbine wheels. The lean of the radial turbine wheel is about 18° and for the mixed flow turbine wheel, it is about 33°. Figure 4(i) and (ii) shows the side views of both the RFVGT and MFVGT geometries (a and b) corresponding to maximum and minimum opening positions of nozzle vanes. These positions are achieved by the movement of an actuator-kinematic system specially designed for this purpose.

The nozzle vanes are arranged in a sub-assembly called cartridge assembly. The cartridge assembly consists of the nozzle vanes, the inner and outer vane bearings and the unison ring or the actuating

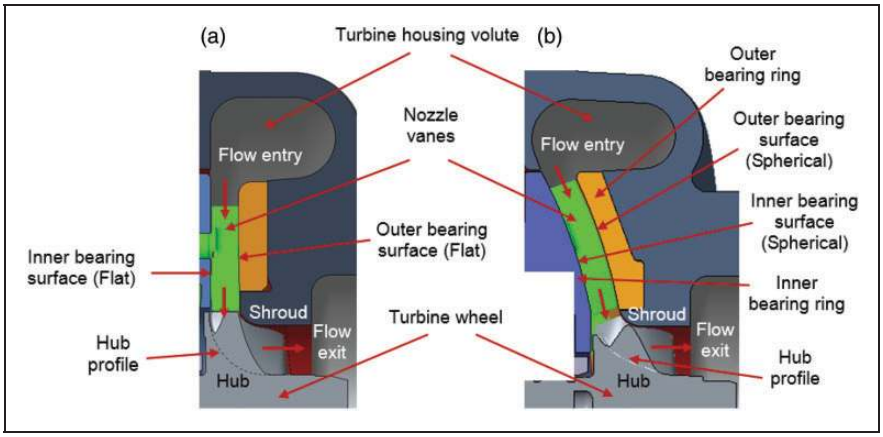

Figure 2. Turbine stage for RFVGT and MFVGT: (a) radial flow VGT; and (b) mixed flow VGT.

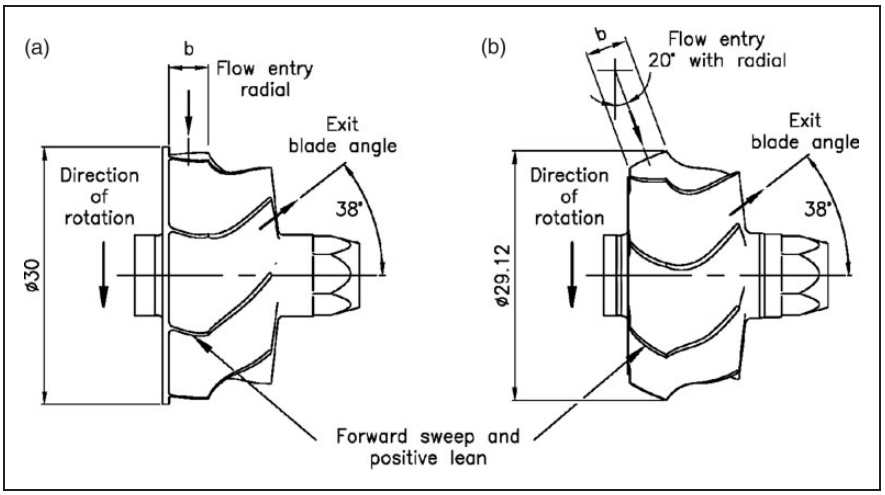

Figure 3. Schematic of the radial flow and mixed flow turbine wheel geometry: (a) radial flow turbine wheel; and (b) mixed flow turbine wheel.

ring. The nozzle vanes are fixed on one end of the spindle shaft, cast as a single piece. The other end of the spindle is connected with inner lever. The inner levers with the same number as the vanes, are arranged inside the actuating ring, which has the slotted provision to actuate the levers circumferentially to the required angular sector. This circumferential movement is enabled with the help of pneumatic/electrical actuator. The actuating rod provides the rotational movement to inner lever, which in turn is connected with the vane spindle causing rotation of nozzle vanes. Thus, closing and opening of the nozzle vanes is achieved. The level of circular movement of the adjusting ring determines the opening position of the vanes.

The difference in the maximum to minimum nozzle vane opening is termed as vanes movement range. This range is 37.4° for the RFVGT and 49.9° for the MFVGT. The higher range for MFVGT is achievable due to the space realized due to spherical surface. At maximum opening position, the flow area realized with RFVGT is 337 mm^2 and with MFVGT, it is 423 mm^2. For both VGTs, the minimum opening area is fixed to 22.6 mm^2 for common reference purpose. The turbocharger assembly is made together with bearing system and compressor. For both RFVGT and MFVGT, the compressor specification remains the same with compressor wheel having tip diameter of 32.5 mm. The internal parts specifications of the bearing system, including the shaft, journals, thrust bearing, and flinger sleeve, are also the same for the both.

Experimental set-up

For analyzing the turbine stage performance during the steady-state condition, experiments are conducted at Turbo Energy Private Limited, Chennai on a turbocharger test rig specially developed for testing the turbocharger with cold air. The layout of the turbocharger cold air test rig is shown in Figure 5. The use of an actual compressor as a loading device offers a wider speed range using cold or hot gas as a turbine-driving medium with speeds up to 300,000 r/min. At delivery to the compressor, a valve is installed to create the back pressure at compressor

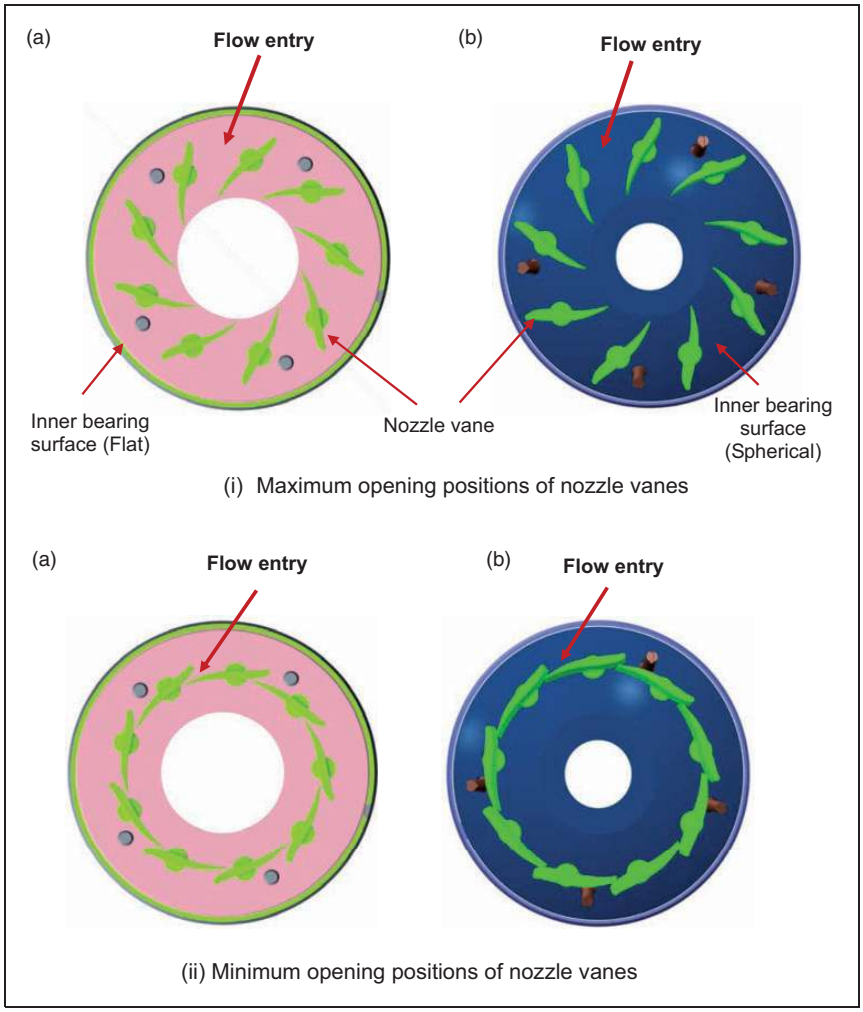

Figure 4. Side views of the (a) RFVGT and (b) MFVGT geometries at maximum and minimum opening positions of nozzle vanes.

outlet and hence loading the turbine. This enables wider operating flow regime for the turbine, without compressor surging.

An oil-free, screw-type air compressor having a flow capacity of 0.265 m^3/s at 3.5 bar (g) is used for supplying air to the cold air turbocharger test rig. The delivery air pressure of the constant speed air compressor is adjusted according to the flow requirement of the turbine to achieve required turbine speeds and expansion ratios. The required amount of air flow at desired pressure is supplied to the turbine through a set of flow control valves namely by-pass valve and turbine inlet flow/pressure control valve. The compressed air temperature, which is proportional to the compressed air delivery pressure, varies from 50 °C at lower pressure to 120 °C at higher pressure of about 2.5 bar (g). This temperature is sufficiently higher for having the air temperature after the expansion above the ambient temperature at any point of the time during testing, to avoid the formation of the condensation during expansion of air in the turbine. There is no heat exchanger installed in the air supply line. Hence, maintaining constant temperature is not feasible under current test set-up, for different speeds and pressure ratios.

Mass flow through the turbine is measured by an orifice meter having 35 mm diameter with D-D/2 tapping set up and mas flow though the compressor is measured using convergent type nozzle with 25 mm diameter, both designed according to the BS1042[19] standard. All the temperatures are measured using grounded junction "K" type (Chromel-Alumel) thermocouples and the pressures are measured by using the pressure transmitters with 4–20 mA output. The turbocharger rotor speed is measured using the "PICOTURN" make inductance type speed sensor. All the measured parameters are logged through a high frequency data logger with data acquisition sampling rate of 50 Hz. The uncertainty in measurement of pressure and temperature is about ±1.5% for the typical turbine inlet flow condition at 1 bar (g) and 90 °C. The conditioned oil to the required temperature and the pressure is supplied to the turbocharger bearing system using lubricating oil power pack system, which has the provision for heating and cooling of oil.

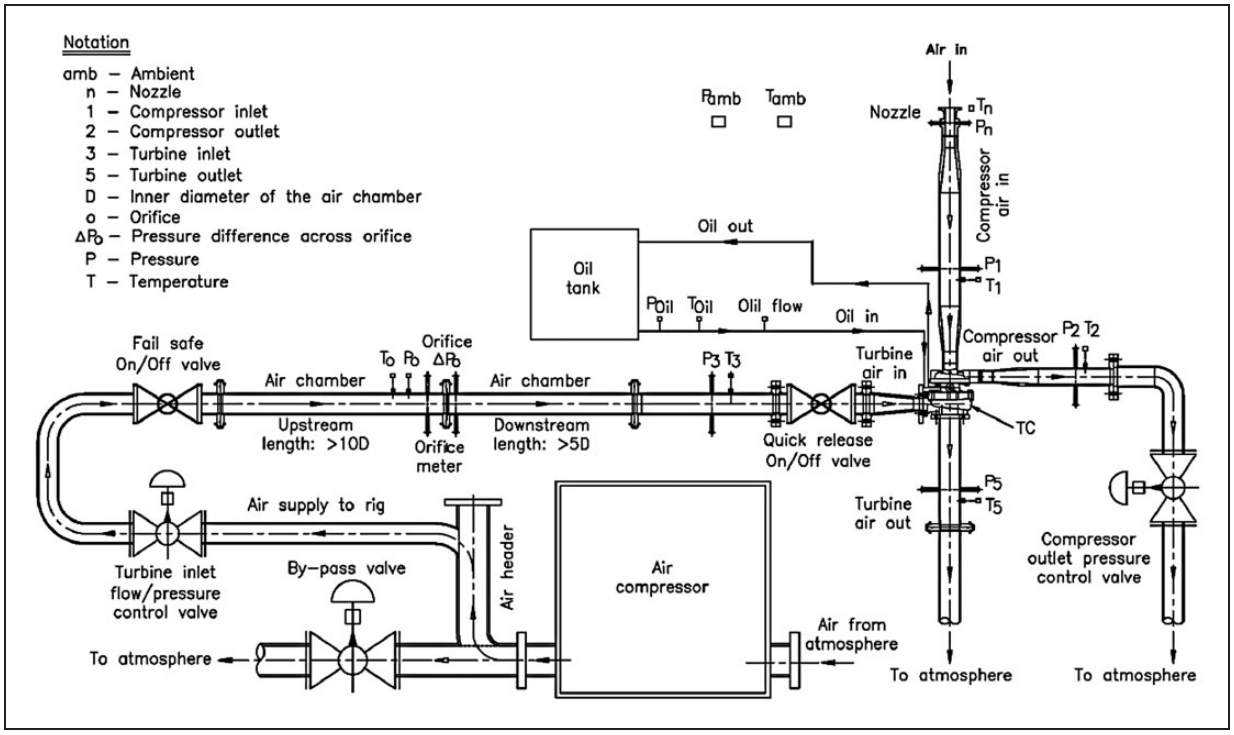

Figure 5. Turbocharger cold air test rig layout.

Experiments

The experimental tests are carried out in two combinations. First, generating the data for both RFVGT and MFVGT configurations for the dimensionless performance parameters: mass flow parameter (MFP), speed parameter, and expansion ratio in their full ranges. Second, the MFP is kept almost the same for both the configurations and the data are generated to compare both the configurations. The first is prescribed in the following, whereas the second is taken up in the next sub section.

Test procedure for comparison of mass flow parameter

Compressed air is made to pass through the turbine at chosen values of inlet pressure, flow rate, and rotational speed. The nozzle vanes are operated from the maximum (refer Figure 4(i)) to the minimum (refer Figure 4(ii)) opening positions and thus varying the nozzle flow area. The tests are conducted at different speeds and expansion ratios. The measured values of turbine MFP are plotted against turbine expansion ratio for different test runs. The expansion ratio and the turbine MFP are defined as follows

$$\text{Expansion Ratio} = \frac{P_{03}}{P_{5s}} \tag{1}$$

$$\text{Turbine mass flow parameter, MFP} = \frac{m_T \sqrt{T_{03}}}{P_{03}\, A^*} \tag{2}$$

A reference expansion ratio is arbitrarily chosen, close to the maximum MFP and for the maximum opening position (in this case, the expansion ratio is 2.2). This is indicated by m_1. At the same expansion ratio, the MFP for the minimum opening position, m_2, is obtained. The difference in MFP $(m_1 - m_2)$, is called the range of MFP. In order to conduct experiments across the range of turbine MFP, the quantity $(m_1 - m_2)$ is divided into four equal parts and the intermediate MFP values are termed 25%, 50%, 75% of the MFP. During testing, the vane position is determined for each of these intermediate MFP values and the corresponding nozzle opening positions are locked by using the external actuator-kinematic system. As mentioned earlier, tests are conducted for different speeds and expansion ratios at these five opening positions. Corresponding to each lever position (part of the actuator-kinematic system), the area of opening of the nozzle vanes is geometrically estimated. Figure 6 shows the performance of RFVGT for different opening positions of nozzle vanes. In Figure 6, at a chosen expansion ratio of 2.2, the maximum and minimum MFP values are marked as m_1 and m_2. The intermediate values of 75%, 50%, and 25% are also identified in the Figure 6. The images of the nozzle vanes opening position is also given as insert in Figure 6. Also, a similar method is followed for MFVGT, but not shown.

For the purpose of reference, the geometric flow area at the opening position of minimum nozzle vanes is fixed as 22.6 mm^2, for both the RFVGT and MFVGT configurations. However, certain level of further nozzle vane opening is required to

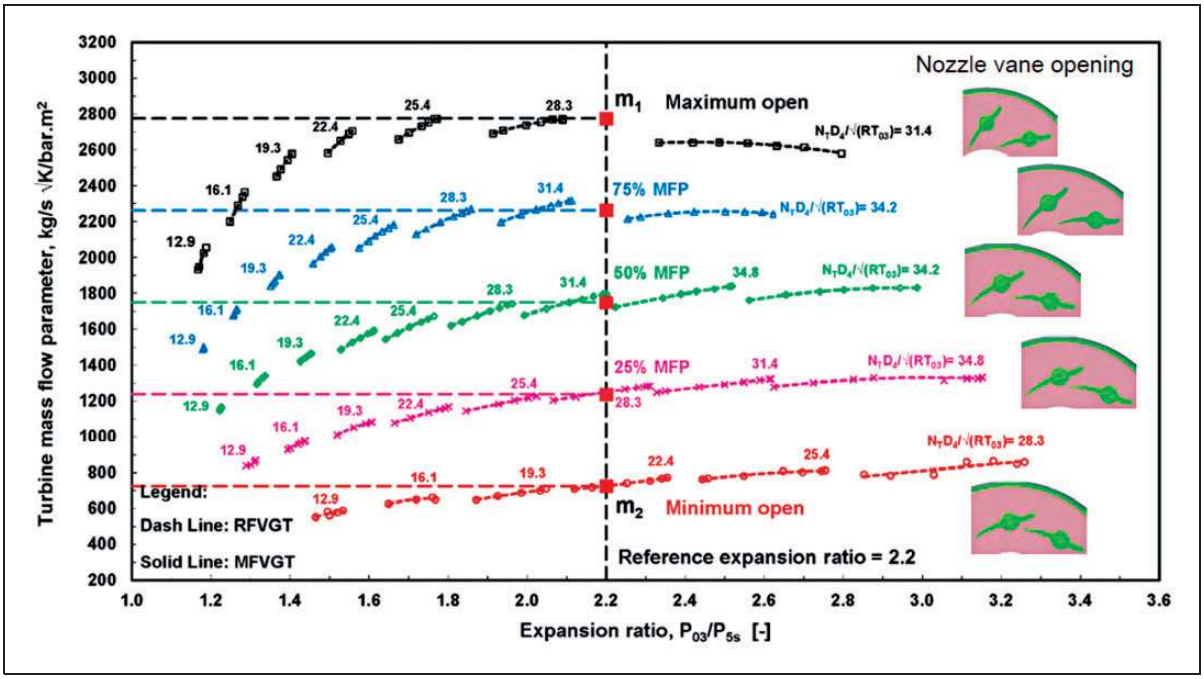

Figure 6. Performance of RFVGT at different opening positions of nozzle vanes.

achieve flow stability in the turbine at different speed parameters and expansion ratios. Such opening position of the nozzle vanes is referred as minimum opening position, which is obtained by experimentally observing the occurrence of stable flow. In RFVGT, the nozzle area for minimum opening position is about 80 mm^2 and for the MFVGT, it is about 50 mm^2.

The steady-state performance test is conducted at different opening positions of nozzle vanes, from maximum to minimum, at different turbine constant speeds and expansion ratios. During testing, the lubricating oil pressure and temperature for turbocharger rotor is maintained at 4 ± 0.2 bar (g) and $90 \pm 5\,^{\circ}C$ respectively. For every turbocharger speed, the turbine is loaded by varying the compressor delivery air pressure from minimum to maximum level. The minimum flow rate is limited to a value at which a stable flow occurs through the compressor, before the onset of surge. During tests, the rotor speed parameter is maintained constant by adjusting the turbine inlet pressure and the mass flow rate.

During the cold tests, the turbine inlet temperature is varied from $50\,^{\circ}C$ to $120\,^{\circ}C$, while the turbine casing is insulated. However, between MFVGT and RFVGT, for same turbine speed level, the difference in temperature variation is about $\pm 5\,^{\circ}C$ as shown in Table 3. The heat transfer effects, if any, are therefore similar for both MFVGT and RFVGT.

In order to compare the performance of the MFVGT and RFVGT on a common ground, the effect of diameter (geometry) and turbine inlet temperature are brought together by using the dimensionless speed parameter (N^*) instead of the directly measured turbine speed (N_T). The dimensionless speed parameter is defined as

$$N^* = \frac{N_T\, D_4}{\sqrt{RT_{03}}} \tag{3}$$

where N_T is the turbine speed (r/min), D_4 is the turbine wheel tip diameter (m), R is the characteristics gas constant for the turbine inlet air (J/kg K), and T_{03} is the turbine total inlet air temperature (K).

Table 4 shows the list of parameters and their ranges measured during testing.

Test procedure: For tests under similar mass flow parameter conditions

In order to conduct these tests, the RFVGT conditions and opening positions are kept as a reference at a chosen expansion ratio. The MFVGT opening is changed in such a way that the MFP is brought as close to the RFVGT value as possible at the same expansion ratio. These conditions are maintained for the maximum, 75%, 50%, and 25% MFP values corresponding to RFVGT. The MFP values maintained similar between both configurations are close to: 2775, 2263, 1750, and 1238 kg/s $\sqrt{K}$/bar m^2. It is to be mentioned that in general, relatively more closing of vane positions is required to bring the MFP of MFVGT closer to that of RFVGT. Therefore, it was not possible to bring down the MFP values of MFVGT closer to those of RFVGT for minimum opening position of the latter to sustain stable flow conditions. The tests are

conducted at various conditions after locking the vane positions at the chosen expansion ratio.

Results and discussion

The turbine performance parameters, the turbine MFP, the combined turbine efficiency, the velocity ratio, and the turbine specific speed are discussed. The two operating points corresponding to the expansion ratio of 1.5 and 2.2 are considered for the discussion of turbine performance. The above two operating points represent the engine conditions closer to the lower and higher engine speeds respectively in the actual application, covering the turbine operating range.

Turbine mass flow parameter for RFVGT and MFVGT

The dashed and solid lines in Figure 7 indicate the performance curves of RFVGT and MFVGT, respectively at different opening positions of the nozzle vanes. Each curve is indicated by the respective speed parameter. The colors of the curves indicate the opening positions of the vanes. Table 5 shows the comparison of MFP at two expansion ratios, 1.5 and 2.2, between RFVGT and MFVGT. The turbine MFP of the MFVGT is about 13% higher than the RFVGT at maximum nozzle vane opening position.

At maximum nozzle opening position, the turbine MFP is attaining a plateau; but beyond the expansion ratio of 2.2, the MFP value decreases slightly. For the minimum open position; the MFP is attaining a plateau, little beyond the expansion ration of 2.4. This value of the MFP plateau indicates that the flow chokes beyond the particular expansion ratio for the given position of nozzle vanes opening. Further, it is noticed that for the given opening position of nozzle vanes, the MFVGT is capable of handling higher MFP than the RFVGT for the same expansion ratio. The lower expansion ratio for the given MFP indicates that the resistance to the flow in MFVGT is lower compared to RFVGT for the given engine exhaust mass flow rate. Lower flow resistance in turbine reduces the backpressure in the engine exhaust manifold (pressure before turbine inlet).

This contributes for the lower pumping losses and hence improvement in brake specific fuel consumption and thermal efficiency of the engine. The higher MFP at lower expansion ratio in MFVGT confirms its downsizing potential. Also, the reduction in turbine wheel size for the given turbine configuration without compromising the flow handling capacity, is likely to improve the transient response due to reduction in mass of the turbine wheel and inertia.

Referring to Figure 7, in order to achieve a speed parameter of 16.1 with speed of 100,000 r/min, at minimum nozzle opening position, the expansion ratio for RFVGT is about 1.7. In MFVGT, the same turbine speed is achieved with the speed parameter of 15.6 at a lower expansion ratio of about 1.62, about 4.7% lower than the RFVGT. The same speed parameter is achieved at expansion ratio of about 1.42, 1.32, and 1.26 for 25%, 50%, and 75% MFP openings respectively for RFVGT. For MFVGT, speed parameter

Table 3. Turbine inlet temperature between MFVGT and RFVGT at different turbine speeds.

	Difference in turbine inlet temperature between MFVGT and RFVGT (°C)			
TC speed (r/min)	Maximum open	75% MFP	50% MFP	25% MFP
80,000	3.3	3.4	2.0	
100,000	3.5	4.1	1.6	2.6
120,000	4.1	5.1	2.0	2.2
140,000	3.4	2.9	2.6	0.6
160,000	2.5	1.0	0.0	4.1
180,000	−0.3	−0.3	−1.8	5.2
200,000	5.3	−4.0	−4.0	
220,000		−0.3	−4.8	

MFVGT: mixed flow variable geometry turbine; RFVGT: radial flow variable geometry turbine.

Table 4. List of TC parameters measured.

Measuring parameters	Range
Turbocharger – rotor speed, N_{TC}	0–320,000 r/min
Ambient (P_{amb}) and compressor inlet pressure (P_1)	0–1200 mbar (a)
Pressure at turbine inlet (P_3), compressor outlet (P_2), and before orifice (P_o)	0–4 bar (g)
Pressure at turbine outlet (P_4)	0–1 bar (g)
Pressure drop a across nozzle (ΔP_n) and orifice (ΔP_o)	0–1000 mm WC
Temperature at turbine inlet (T_3) and outlet (T_5), compressor inlet (T_1) and outlet (T_2), before orifice (T_o), near nozzle (T_n), ambient (T_{amb}), and lubricating oil (T_{oil})	−250 °C to +1200 °C

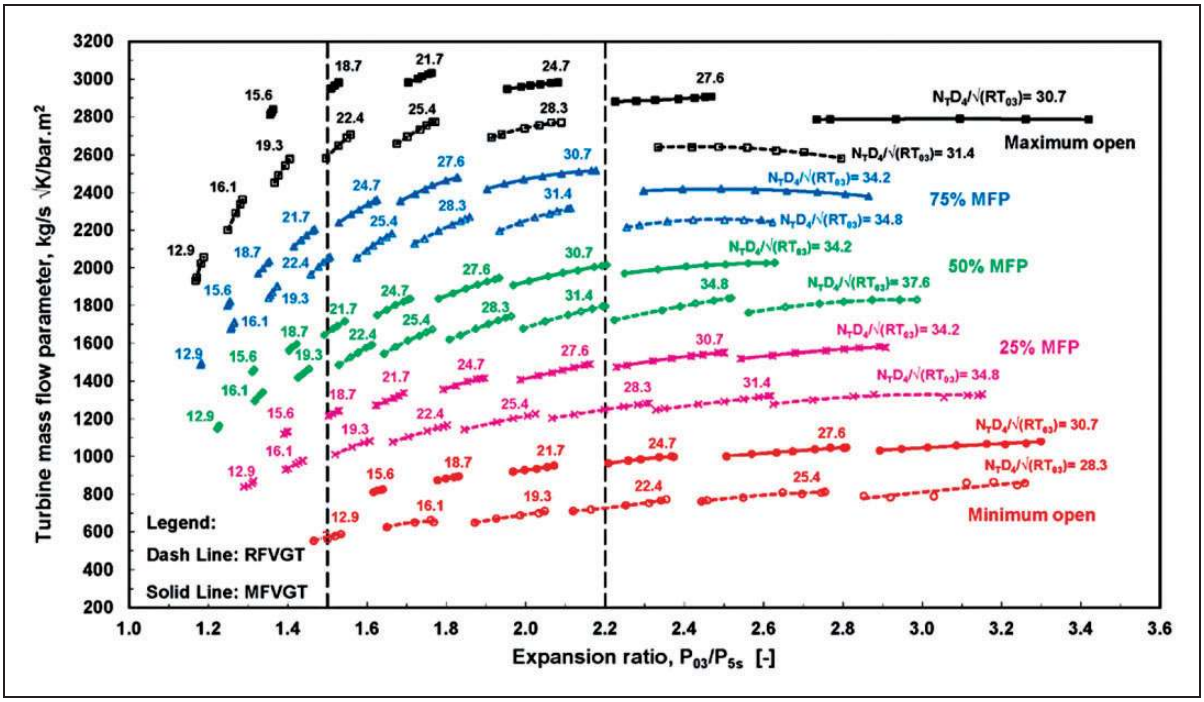

Figure 7. Turbine mass flow parameter vs. expansion ratio for RFVGT and MFVGT at different opening positions of nozzle vanes. MFVGT: mixed flow variable geometry turbine; RFVGT: radial flow variable geometry turbine.

Table 5. Comparison of turbine mass flow parameter: MFVGT vs. RFVGT.

	Turbine mass flow parameter (MFP)					
	At expansion ratio: 1.5			At expansion ratio: 2.2		
Nozzle vanes opening corresponding to	RFVGT (kg/s $\sqrt{K}$/bar m^2)	MFVGT (kg/s $\sqrt{K}$/bar m^2)	Increase in MFP (%)	RFVGT (kg/s $\sqrt{K}$/bar m^2)	MFVGT (kg/s $\sqrt{K}$/bar m^2)	Increase in MFP (%)
Maximum	2600	2940	13.08	2775	2970	7.03
75% MFP	2050	2225	8.54	2263	2465	8.95
50% MFP	1480	1660	12.16	1750	1960	12.00
25% MFP	1010	1210	19.80	1238	1455	17.58
Minimum	575	760	32.17	725	950	31.03

MFVGT: mixed flow variable geometry turbine; RFVGT: radial flow variable geometry turbine.

15.6 is achieved at expansion ratios of about 1.39, 1.3, and 1.25 for 25%, 50%, and 75% MFP openings respectively. At maximum opening position, the speed parameter of 16.1 (100,000 r/min) is achieved at an expansion ratio of about 1.28 for the RFVGT. With MFVGT, the speed parameter of 15.6 (100,000 r/min) is achieved at slightly higher expansion ratio of about 1.35. To maintain a particular turbine speed with increased MFP, the expansion ratio decreases up to 75% MFP of nozzle vane opening and increases thereafter.

The effect of speed parameter on the MFP for three different nozzle vane opening positions is plotted in Figure 8(a) to (c), respectively. It is evident from these figures that for all opening positions and at all speed parameters, the MFP are larger for MFVGT compared to RFVGT.

Comparison of MFVGT and RFVGT under similar MFP

Figure 9 shows the turbine MFP for both the RFVGT and MFVGT with matching the MFPs. As a result of matching the MFP, the performance curves of both the configurations are brought closer to each other. The performance parameters of both the configurations, namely, the combined turbine efficiency, velocity ratio, and specific speed are now comparable and hence are sought to be compared between RFVGT and MFVGT in the next sections.

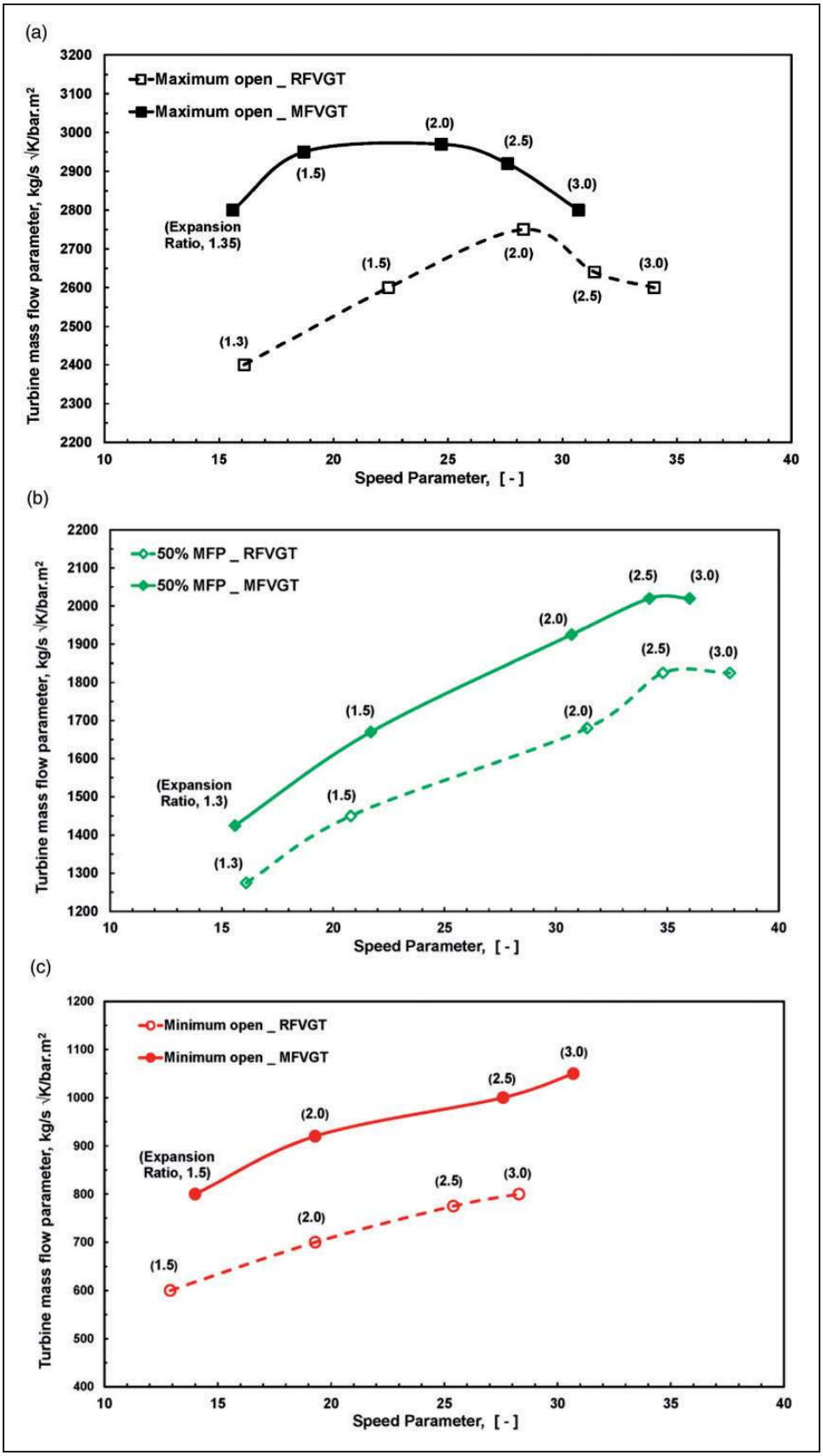

Figure 8. Turbine mass flow parameter vs. turbine speed parameter for RFVGT and MFVGT at different opening positions of nozzle vanes: (a) maximum nozzle vanes open; (b) 50% MFP nozzle vane open; and (c) minimum nozzle vane open.
MFVGT: mixed flow variable geometry turbine; RFVGT: radial flow variable geometry turbine; MFP: mass flow parameter.

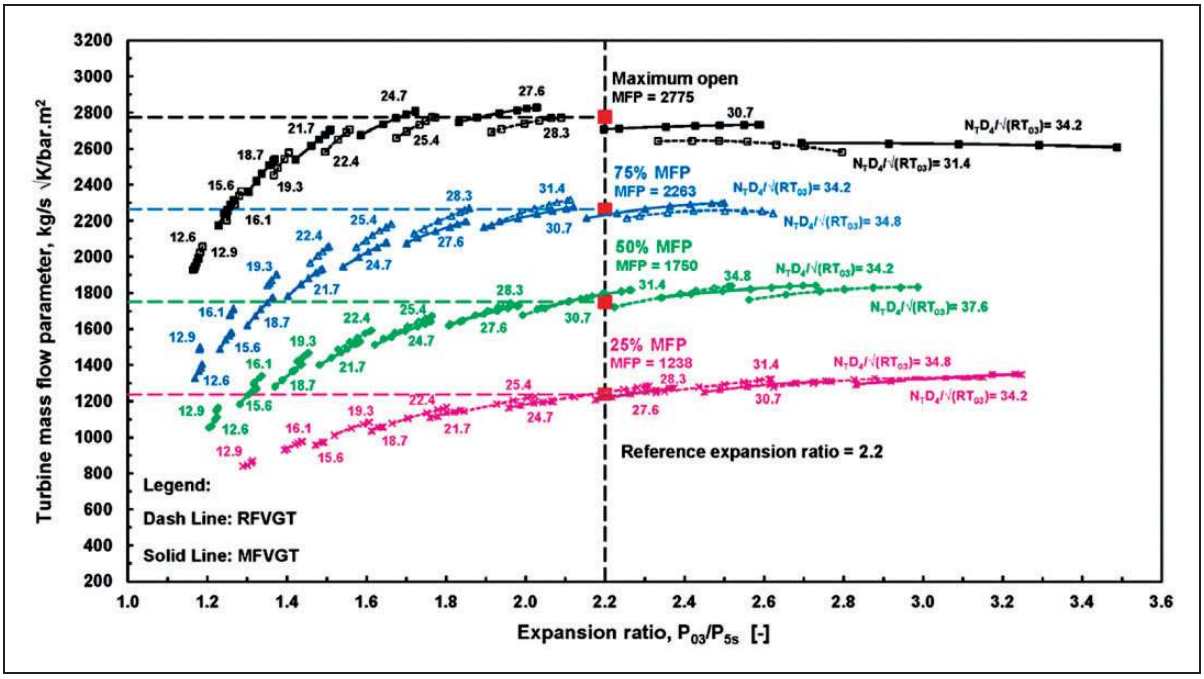

Figure 9. Turbine mass flow parameter vs. expansion ratio for RFVGT and MFVGT at different opening positions of nozzle vanes: similar MFP openings.
MFVGT: mixed flow variable geometry turbine; RFVGT: radial flow variable geometry turbine; MFP: mass flow parameter.

Combined turbine efficiency

The combined turbine efficiency is defined and calculated as follows

$$\eta_{\text{Combined turbine}} = \eta_{\text{Mechanical}} \times \eta_{\text{Turbine}} \tag{4}$$

It is equivalent to the ratio of actual compressor power to the isentropic turbine power

$$\eta_{\text{Combined turbine}} = \frac{P_{C,a}}{P_{T,is}} \tag{5}$$

$$= \frac{m_C\, C_{pa}\,[T_{02} - T_{01}]}{m_T\, C_{pa}\, T_{03}\left[1 - \left(\frac{P_{5s}}{P_{03}}\right)^{\frac{\gamma a - 1}{\gamma a}}\right]} \tag{6}$$

It may be noted that in equation (6), m_C, m_T, T_{01}, T_{02}, T_{03}, and P_{5s} are measured and P_{03} is estimated to obtain the value of the combined turbine efficiency.

Figure 10 shows the comparison of the combined turbine efficiency against the expansion ratio for the RFVGT and MFVGT. Table 6 shows the comparison of combined turbine efficiency at two expansion ratios, 1.5 and 2.2, between RFVGT and MFVGT.

For both the VGTs, Figure 10, it may be noted that the combined turbine efficiency values are higher for 75%, 50%, and 25% MFP. All these values are larger than to values corresponding to 100% MFP (maximum open). Normally, the combined turbine efficiency curve exhibits a drooping behavior showing a maximum at certain expansion ratio. However, in the region of lower expansion ratio and at lower operating speed parameters, the operating range of this expansion ratio is narrow due to the limit of the stable operating domain while loading the compressor. In these range of lower expansion ratios, the combined turbine efficiency characteristics do not exhibit the drooping nature but appear monotonic. This trend that was also observed by Spence and Artt.[20] The operating range might have been improved if the tests were conducted using the hot gas instead of the cold air. Also, Spence and Artt[20] mentioned that the turbine efficiency would probably have shown a maximum had it been possible to test the turbine at higher pressure ratios.

Combined turbine efficiency vs. mass flow parameter

The alternate method of comparing the performance of MFVGT with RFVGT is by analysing the variation of the combined turbine efficiency (the combined turbine efficiency ratio $= \eta_{\text{CT, MFVGT}}/\eta_{\text{CT, RFVGT}}$) over different MFPs for the chosen turbine expansion ratios of 1.5, 2.0, and 2.5. Figure 11 shows this comparison. The error bar is introduced and the uncertainty is higher with the lower expansion ratio. This could be due to the limitation in the range of the turbine loading and unstable operation with lower speeds as described in the previous section.

The advantage of using MFVGT is conspicuous at lower expansion ratio and lower MFPs. Typically, the ratio is more than 2 when the turbine mass flow parameter is less than 1500 kg/s $\sqrt{\text{K}}$/bar m^2 at an expansion ratio of 1.5. On the other hand, the performance of

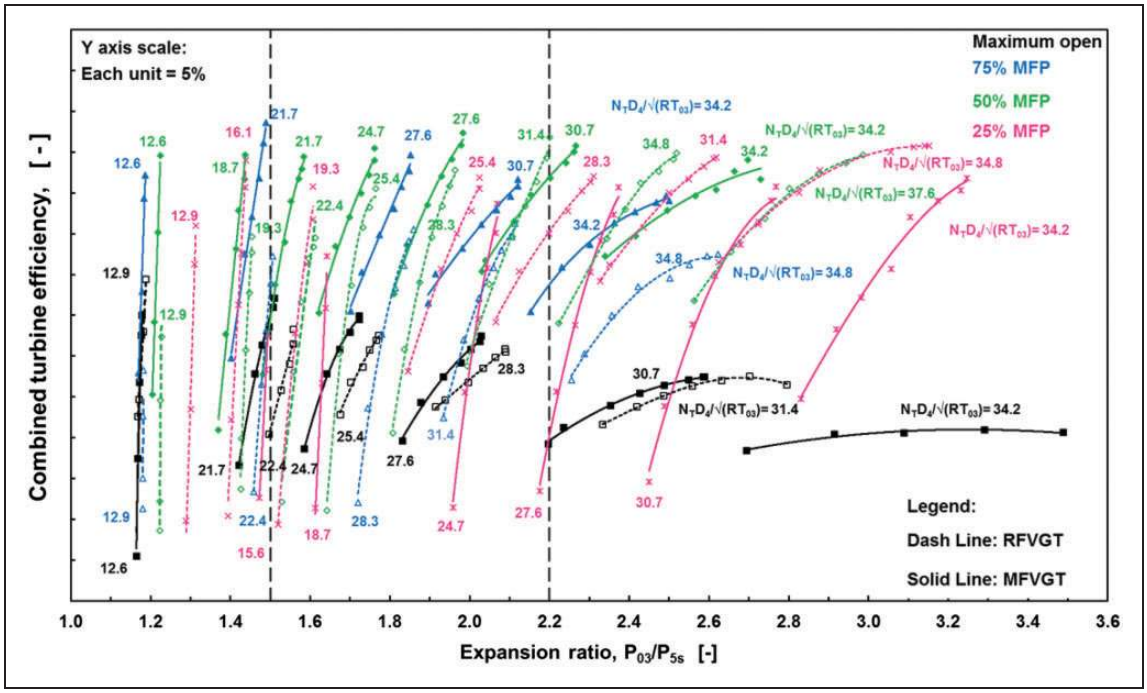

Figure 10. Combined turbine efficiency vs. expansion ratio for RFVGT and MFVGT at different opening positions of nozzle vanes: similar MFP openings.
MFVGT: mixed flow variable geometry turbine; RFVGT: radial flow variable geometry turbine; MFP: mass flow parameter.

Table 6. Comparison of combined turbine efficiency: MFVGT vs. RFVGT.

Nozzle vanes opening corresponding to	Combined turbine efficiency					
	At expansion ratio: 1.5			At expansion ratio: 2.2		
	RFVGT	MFVGT	Increase in eff.	RFVGT	MFVGT	Increase in eff.
Maximum	0.210	0.350	0.140	0.175	0.196	0.021
75% MFP	0.390	0.600	0.210	0.240	0.386	0.146
50% MFP	0.090	0.345	0.255	0.555	0.520	−0.035
25% MFP	0.090	0.360	0.270	0.330	0.205	−0.125

MFVGT: mixed flow variable geometry turbine; RFVGT: radial flow variable geometry turbine; MFP: mass flow parameter.

MFVGT deteriorates significantly when expansion ratio is more than 2 at lower MFPs. However, the combined turbine efficiency of MFVGT is about 25% more than RFVGT at MFPs higher than 2000 kg/s $\sqrt{K}$/bar m^2 for all expansion ratios.

The better turbine performance at lower MFP region translates to faster turbine transient response. This is important for achieving the engine performance with meeting the air flow demand as required during the engine acceleration condition and hence the achievement of transient response of the engine. Normally, the time period for the turbine operation under maximum opening position is relatively less compared to partial MFP condition (varying between maximum opening to minimum opening condition) during vehicle operating condition since the continuous rated power operation of the engine is limited due to traffic pattern and the vehicle driving-duty cycle. However, in order to achieve higher combined turbine efficiency at higher expansion ratios with MFVGT, further optimization may be required. The maximum potential of the MFVGT may be explored with further optimization on the turbine wheel, nozzle vanes and turbine housing volute structure individually.

Velocity ratio

Figure 12 shows the comparison of the combined turbine efficiency against the velocity ratio (U_4/C_0) for the RFVGT and MFVGT. The velocity ratio is defined as follows

$$\text{Velocity ratio, } \frac{U_4}{C_0} = \frac{U_4}{\sqrt{2C_{pa}\ T_{03}\left[1-\left(\frac{P_{5s}}{P_{03}}\right)^{\frac{\gamma a-1}{\gamma a}}\right]}} \quad (7)$$

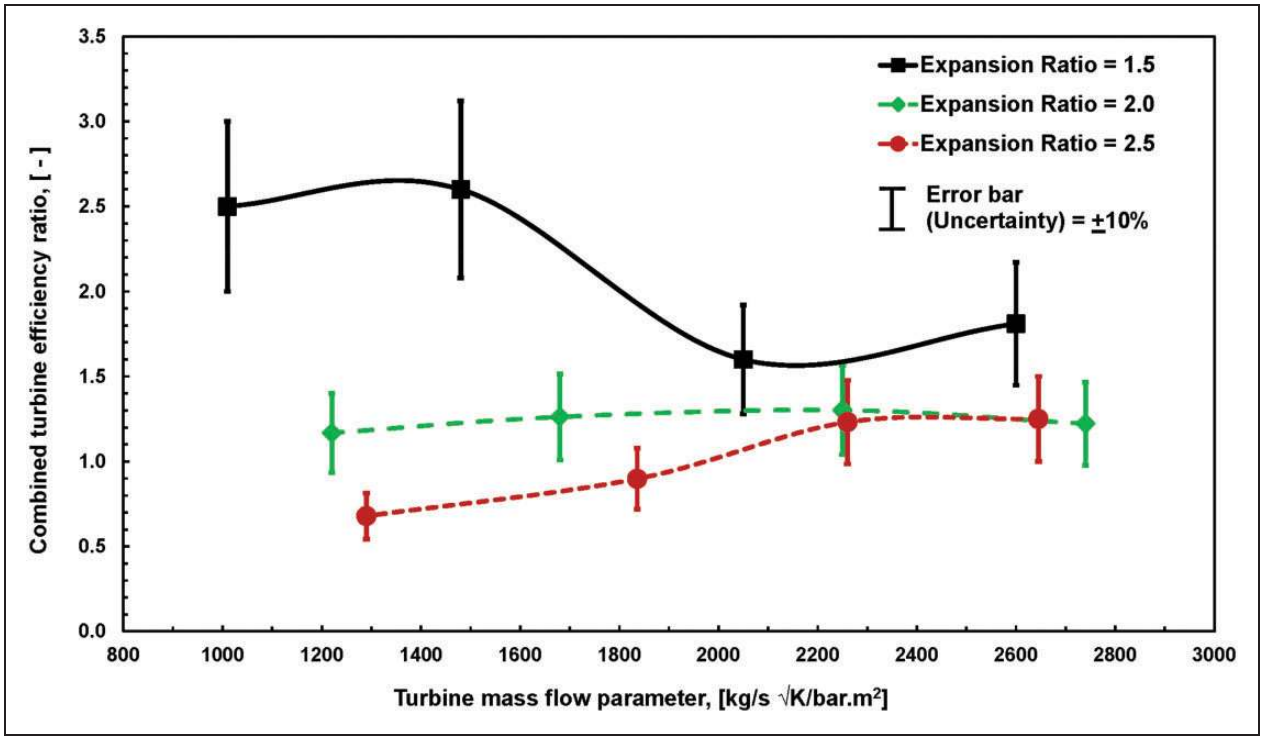

Figure 11. Ratio of combined turbine efficiency vs. turbine mass flow parameter at different expansion ratios for RFVGT and MFVGT (at different opening positions of nozzle vanes: for similar MFP openings).

For both the VGTs (Figure 12), it may be noted that velocity ratio values are progressively higher for 25%, 50%, and 75% MFP. At the maximum opening position, however, the velocity ratio values are lower and closer to 50% MFP. The velocity ratio at which the peak of the combined turbine efficiency occurs with MFVGT is about 0.78. This occurs for a wide operating regime of MFVGT that corresponds to 50% to 75% MFP. However, the corresponding velocity ratio at which the peak efficiency is noticed for RFVGT is 0.83. In contrast to MFVGT, this occurs in a range for RFVGT at around 50% MFP. The range of the velocity ratio for both configurations at the maximum opening position, covering the maximum to minimum speeds, lies between 0.70 to 0.83, a relatively narrow range. The range, however, is wider (between 055 and 0.88, as in Figure 12) for other nozzle vane opening positions. The maximum combined turbine efficiency is observed at nozzle vanes opening corresponding to 50% MFP. According to Spence and Artt,[20] the flow throat area in the nozzle vanes (stator) and turbine wheel (rotor) seems to be optimum at 50% MFP opening and can be considered as the design point for the turbine stage.

It may be noticed that with the mixed flow turbine wheel, the higher level of positive blade angle at turbine wheel entry contributes for the lower velocity ratio. This leads to the occurrence of maximum design point efficiency at relatively lower velocity ratio with MFVGT (mixed flow turbine wheel) than the RFVGT (radial flow turbine wheel). This indicates that the MFVGT has a higher combined turbine efficiency even at higher expansion ratio. Considering the above, the MFVGT is more suitable for the turbocharger application over the entire engine operating conditions.

Turbine specific speed

Figure 13 shows the comparison of the combined turbine efficiency against the turbine specific speed for the RFVGT and MFVGT. The turbine specific speed is defined as follows

$$\text{Turbine specific speed, } Ns = \frac{\omega\sqrt{Q_T}}{\Delta h_0^{3/4}} \tag{8}$$

The turbine specific speed at which the maximum combined turbine efficiency occurs with MFVGT is about 0.88 and occurring at 75% MFP position. In RFVGT, it is about 0.73 and occurring at 50% MFP position. At 25% MFP position, the specific speed for the peak efficiency of the MFVGT is about 0.58 against the RFVGT with 0.56. At nozzle vanes opening corresponding to 50% MFP, the specific speed for the peak efficiency is about 0.74 for both the RFVGT and MFVGT. However, at higher flow regions of every turbine speed parameter, the specific speed for MFVGT is higher than the RFVGT for the corresponding speed parameters. This indicates that the energy utilization in MFVGT is higher than the

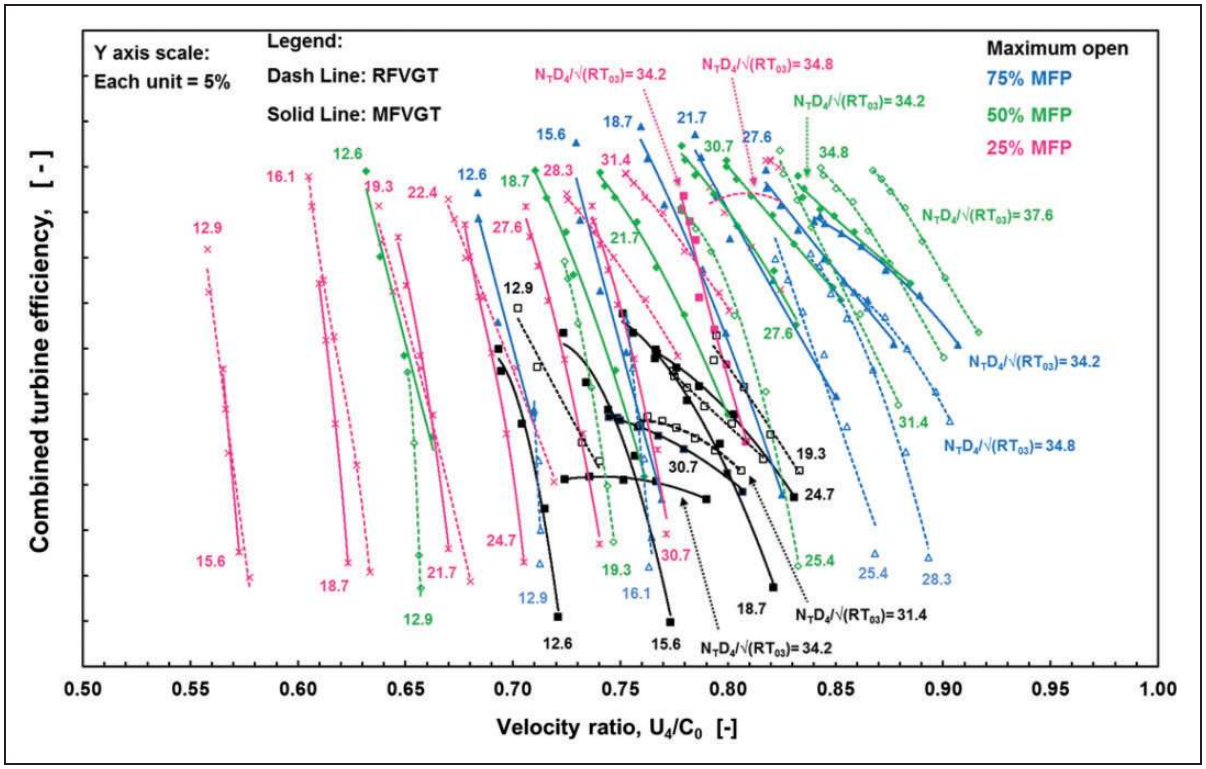

Figure 12. Combined turbine efficiency vs. velocity ratio for RFVGT and MFVGT at different opening positions of the nozzle vanes: similar MFP openings.
MFVGT: mixed flow variable geometry turbine; RFVGT: radial flow variable geometry turbine; MFP: mass flow parameter.

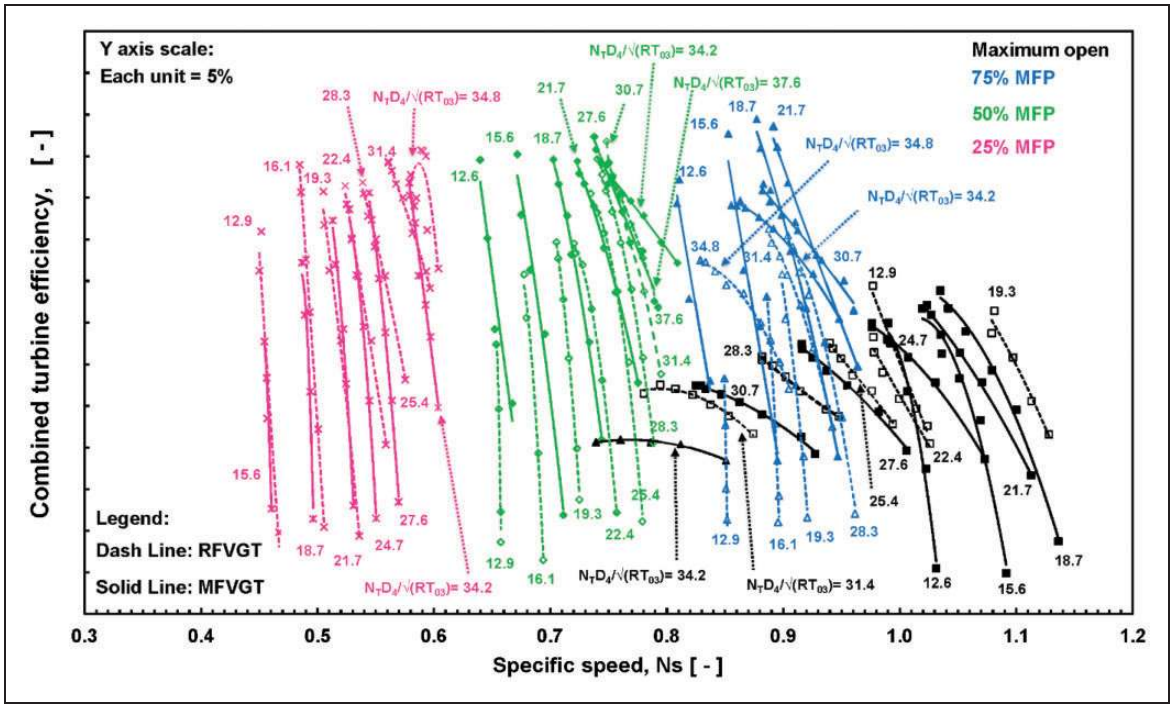

Figure 13. Combined turbine efficiency vs. turbine specific speed for RFVGT and MFVGT at different opening positions of nozzle vanes: similar MFP openings.
MFVGT: mixed flow variable geometry turbine; RFVGT: radial flow variable geometry turbine; MFP: mass flow parameter.

RFVGT for the given input energy. At nozzle vanes opening corresponding to maximum, the specific speed for the peak efficiency of the MFVGT is about 1.04 against the RFVGT with 0.98. The specific speed increases with MFP for both the MFVGT and RFVGT.

Conclusions

In this research, a new mixed flow variable geometry turbine is developed for the turbine wheel size of about 30 mm. The performance of the mixed flow variable geometry turbine is compared with the radial flow variable geometry turbine through experimental analysis. The salient conclusions obtained from the work are summarized as follows.

The turbine MFP of the MFVGT is about 7 to 13%, 12%, and about 32% (refer to Table 5) higher than the RFVGT respectively for the nozzle vanes opening corresponding to maximum open, 50% MFP and minimum opening position. This indicates that the MFVGT is capable of handling higher turbine MFP compared to RFVGT for the similar rotor size.

For similar turbine MFP condition, at lower expansion ratio of about 1.5, the combined turbine efficiency of the MFVGT is about 14% to 27% higher than the RFVGT. At higher expansion ratio of about 2.2, the combined turbine efficiency of the MFVGT is about 2% and 14.6% higher than the RFVGT respectively for nozzle vanes opening corresponding to maximum open and 75% MFP. In 50% to 25% MFP region, the combined turbine efficiency of the MFVGT is about 3.5% and 12.5% respectively lower than the RFVGT.

At the nozzle vanes opening position corresponding to 50% MFP and 75% MFP, the velocity ratio at which the peak combined turbine efficiency occurs with MFVGT is lower. The value of velocity ratio for MFVGT is 0.78 against the 0.83 with RFVGT. In MFVGT, the maximum combined turbine efficiency is observed at nozzle vanes opening corresponding to 50% MFP to 75% MFP. However, in RFVGT, the maximum combined turbine efficiency occurs at nozzle vanes opening corresponding to 50% MFP. This indicates that for the wide MFP region, the combined turbine efficiency is higher in MFVGT compared to RFVGT.

The turbine specific speed at which the maximum combined turbine efficiency occurs with MFVGT is about 0.88 and for the RFVGT is about 0.73. Higher level of combined turbine efficiency is observed with MFVGT compared to RFVGT.

The test results thus provide clear evidence of higher mass flow handling capacity and higher combined turbine efficiency with MFVGT compared to RFVGT for the similar turbine size.

Albeit a minor reduction is combined turbine efficiency at higher expansion region at 25% and 50% MFP openings, a higher level of combined turbine efficiency is observed in other mass flow and expansion ratio regions with MFVGT compared to RFVGT. This in turn confirms the potential of MFVGT for higher mass flow handling capacity with higher combined turbine efficiency at lower expansion ratios region, which is more desirable for the engine operation and transient conditions.

Acknowledgements

The authors are sincerely grateful to M/s. Turbo Energy Private Limited, Chennai, for supporting the research, development and testing.

Declaration of Conflicting Interests

The author(s) declared no potential conflicts of interest with respect to the research, authorship, and/or publication of this article.

Funding

The author(s) received no financial support for the research, authorship, and/or publication of this article.

ORCID iD

K Ramesh http://orcid.org/0000-0002-9933-0151

References

1. http://www.ingenia.org.uk/Content/ingenia/issues/issue49/Knopf.pdf (accessed December 2011).
2. Okapuu U. Design and aerodynamic performance of a small mixed flow gas generator turbine. *AGARD* 1987; CP-421: 16-1–16-11.
3. Karamanis N, Martinez-Botas RF and Su CC. Detailed flow measurements at the exit of a Mixed Flow Turbine under steady flow conditions. ASME paper no. 99-GT-342, 1999.
4. Karamanis N and Martinez-Botas RF. Mixed-flow turbines for automotive turbochargers: Steady and unsteady performance. *Int J Eng Res* 2002; 3: 127–138.
5. Baines NC, Wallace FJ and Whitefield A. Computer aided design of mixed flow turbines for turbochargers. *Trans ASME* 1979; 101: 440–448.
6. Roclawski H, Gugau M, Langecker F, et al. Influence of degree of reaction on turbine performance for pulsating flow conditions. ASME paper no. GT2014-25829, 2014.
7. Rajoo S and Martinez-Botas R. Mixed flow turbine research: A review. *ASME-J Turbomach* 2008; 130: 044001: 1–12.
8. Wallace FJ and Pasha SGA. Design construction and testing of a mixed flow gas turbine. In: *The second international JSME symposium on fluid machinery and fluids*, Tokyo, Japan, 1972, pp.213–214.
9. Oh JS, Buckley CW and Agarawal GL. Computational aerodynamic performance and mixed-flow design options for high specific speed turbine. ASME paper no. GT2008-50714, 2008.
10. Ramesh K, Prasad B and Sridhara K. Transient response of mixed flow variable geometry turbine for a turbocharger. ASME paper no. GTINDIA2015-1372, 2015.

11. Baines NC. *Fundamental of turbocharging*. Concepts ETI, Inc. d.b.a. *Concepts NREC* 2005; 92–111.
12. Baines N. Radial and mixed-flow turbine options for high boost turbochargers. In: *Seventh international conference on turbochargers and turbocharging*, 2002, C602/014/2002, pp.35–44. London: Institution of Mechanical Engineers.
13. Rodgers C. The characteristics of radial turbines for small gas turbines. ASME paper no. GT2003-38026, 2003.
14. Cox GD, Fischer C and Casey MV. The application of throughflow optimisation to the design of radial and mixed flow turbines. In: *9th international conference on turbochargers and turbocharging*, Combustion Engines and Fuels Group, 2010, pp.217–226. London: Institution of Mechanical Engineers..
15. Roclawski H, Boehle M and Gugau M. Multidisciplinary design optimisation of a mixed flow turbine wheel. ASME paper no. GT2012-68233, 2012.
16. Li C, Zhuge WL, Zhang YJ, et al. Investigation of the secondary flow structure in the mixed flow turbine for a high pressure ratio turbocharger. ASME paper no. GT2008-50941, 2008.
17. Palfreyman D, Martinez-Botas RF and Karamanis N. Computational and experimental investigation of the aerodynamics of turbocharger mixed flow turbines. In: *Seventh international conference on turbochargers and turbocharging*, 2002, pp.45–59. London: Institution of Mechanical Engineers.
18. He P, Sun ZG, Zhang HL, et al. Investigation of clearance flows in deeply scalloped radial turbines. *Proc IMechE, Part A: J Power and Energy* 2012; 226: 951–962.
19. British Standard Institution. *Methods of measurement of fluid flow in closed conduits*. BS1042, section 1.1, 1981.
20. Spence SWT and Artt DW. Experimental performance evaluation of a 99.0 mm radial inflow nozzled turbine with different stator throat areas. *Proc IMechE, Part A: J Power and Energy* 1997; 211: 477–488.

Appendix

Notation

A^*	turbine wheel exducer throat area (m^2)
A/R	ratio of turbine housing volute flow area and area center with respect to rotor axis (mm)
b	turbine wheel blade width at entry (mm)
C_0	air velocity achieved by isentropic expansion from turbine inlet conditions (m/s)
C_p	specific heat at constant pressure (J/kg K)
d	diameter of the orifice (mm)
D	inner diameter of the air chamber (mm)
m	mass flow rate (kg/s)
m_1	mass flow parameter at maximum nozzle vane opening position (kg/s $\sqrt{\text{K}}$/bar m^2)
m_2	mass flow parameter at minimum nozzle vane opening position (kg/s $\sqrt{\text{K}}$/bar m^2)
N	speed (r/min)
Ns	specific speed
N^*	speed parameter
P	pressure, bar (g)/bar (a) (mbar/mmWC); power
Q	volume flow rate (m^3/s)
T	temperature (°C/K)
U	turbine tip velocity (m/s)
U/C_0	velocity ratio
Δh	specific energy (J/kg)
ΔP	pressure drop (mmWC)
η	efficiency
γ	ratio of specific heats
ω	rotational speed (rad/s)

Subscripts

0	total condition
1	compressor inlet condition
2	compressor outlet condition
3	turbine housing inlet condition
4	turbine wheel inlet condition, leading edge
5	turbine outlet condition
a	actual, air
amb	ambient
c	compressed air
C	compressor
CT	combined turbine
is	isentropic condition
n	nozzle
o	orifice
s	static condition
t	tip
T	turbine
TC	turbocharger